Book of Tutorials and Abstracts

European Microbeam Analysis Society

EMAS 2026

15th

REGIONAL WORKSHOP

TOPICAL CONFERENCE ON ELECTRON BACKSCATTER DIFFRACTION (EBSD)

14 to 17 June 2026
at the
CentraleSupélec, Gif-sur-Yvette, France

Organised in collaboration with:
ICMMO, ENS Paris-Saclay,
Université Paris-Saclay

EMAS
European Microbeam Analysis Society eV
www.microbeamanalysis.eu/

This volume is published by:
European Microbeam Analysis Society eV (EMAS)
EMAS Secretariat
c/o Eidgenössische Technische Hochschule, Department of Earth and Planetary Sciences
Clausiusstrasse 25
8092 Zürich
Switzerland

ISBN 978 90 8227 6992
NUR code: 971 – Materials Science

ORIENTATION REPRESENTATION

Stuart I. Wright*, and W.L. Lenthe

Ametek, Inc., GATAN + EDAX Business Unit
5794 W. Las Positas Blvd., US-94588 Pleasanton, California, U.S.A.
e-mail: stuart.wright@ametek.com

Stuart Wright is a Senior Scientist at Gatan EDAX focussed on Electron Backscatter Diffraction (EBSD). Stuart first got involved with EBSD with the first system in North America installed by David Dingley at Brigham Young University for Brent Adams' research team in 1987. Stuart followed Professor Adams to Yale University where automating EBSD became the core of Stuart's PhD thesis research. The first fully automated EBSD scans were completed in the fall of 1991. After completing his thesis Stuart joined Los Alamos National Lab and continued work in texture analysis.

In 1995 he joined TSL. TSL was founded to commercialise automated EBSD. Stuart fulfilled many roles at TSL but always involved in software development. He has continued in this role through the evolution of TSL to Gatan. Stuart has published over 59 papers in archival journals, two of which have received paper-of-the-year awards, he has over 110 papers in conference proceedings or other publications and 5 patents. Stuart is a frequent speaker at conferences and workshops and reviewer for several archival journals. He has organised EBSD symposia at several conferences, hosted the International Conference on Textures of Materials in 2017 and has been involved with developing EBSD standards and guidelines.

1. *INTRODUCTION*

One of the key objectives of electron backscatter diffraction (EBSD) is to measure crystallographic orientation. Each constituent grain in a polycrystal has a different orientation as schematically illustrated in Fig. 1 for a polycrystalline sample composed of two phases, one with cubic crystal symmetry and a second with hexagonal crystal symmetry.

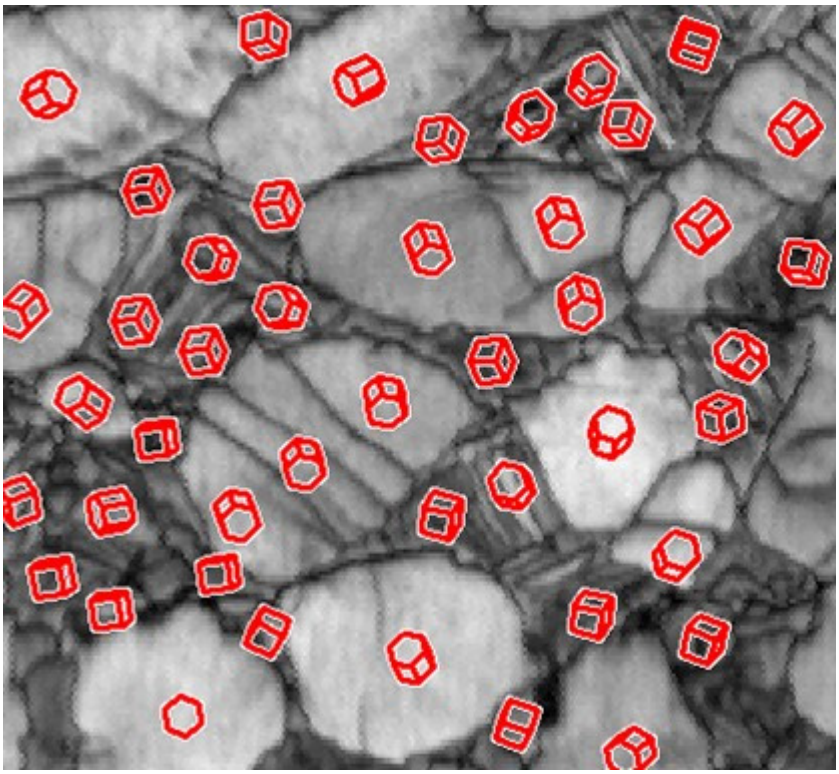

Figure 1. Schematic of crystallographic orientations in a two phase polycrystal.

For this discussion, we assume the reader has some familiarity with the crystallographic notation for planes (*hkl*) and directions [*uvw*] as well as crystal symmetry. If not, we recommend the reader learn of these concepts in crystallographic or metallurgical textbooks or using web-based tools.

2. *CRYSTAL PLANES*

While crystallographic orientation is a three-dimensional (3D) entity, often only the alignment of a crystal plane relative to the sample reference frame is of interest which is only 2D in nature. This is because many material properties are specific to particular lattice planes in the crystal. For example, slip generally happens on specific crystal planes – e.g., {111} planes in face centred cubic materials or basal planes {0001} in hexagonal close-packed materials.

2.1. Pole figures

A common graphical representation of orientation is the pole figure. A pole figure shows the orientation of a specific crystal plane (given by (*hkl*)) with respect to the sample surface. Imagine a sphere surrounding a hexagonal crystal. Consider where the basal pole (i.e., the {0001} plane-normal or <0001> crystal direction) intersects the sphere. The pole figure is the projection of the sphere containing this intersection point onto a two-dimensional plane. The projection of the sphere on to the 2D plane forms a circle. The intersection of the plane normal with the sphere is also projected on to the 2D plane to form a dot as shown in Fig. 2 for a crystal with hexagonal point group symmetry.

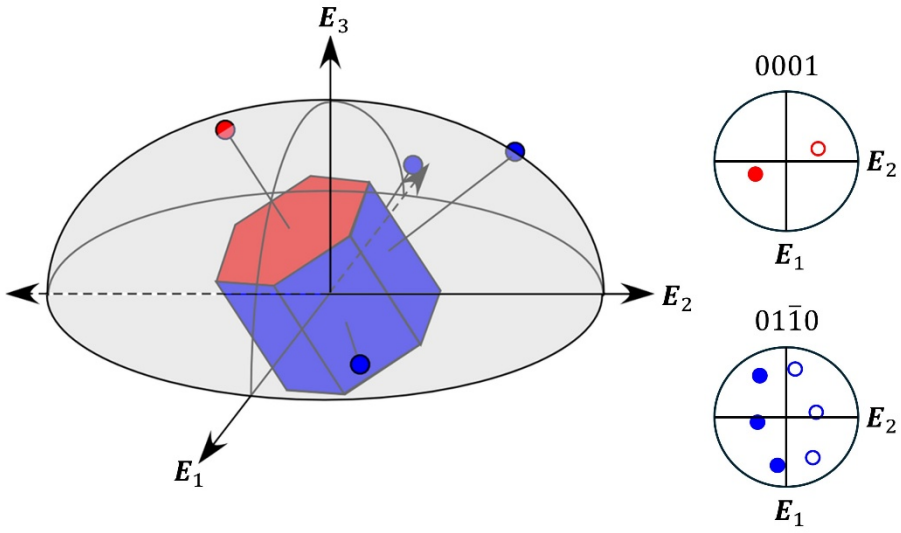

Figure 2. Schematic of pole figure for a single hexagonal crystal.

This can be done for any pole. Two pole figures are shown in Fig. 2, a {0001} and a $\{101\bar{0}\}$ pole figure. First, consider the {0001} pole figure. This pole figure has two dots, one solid and one open. The solid dot corresponds to the (0001) plane up out of the plane of the page (i.e., the upper hemisphere); whereas the open dot corresponds to the $(000\bar{1})$ plane projected down into the plane of the page (i.e., the lower hemisphere). For a hexagonal crystal, the (0001) and $(000\bar{1})$ planes are symmetrically equivalent. (Note that "(*hkil*)" denotes a specific plane whereas "{*hkil*}" denotes a family of symmetrically equivalent planes. Similarly, "[*hkil*]" denotes a specific crystallographic direction, whereas "⟨*hkil*⟩" denotes a family of symmetrically equivalent directions). Generally, pole figures plot only one hemisphere. Metallurgists tend to use the upper hemisphere, whereas geologists tend to use the lower.

Note also that the {0001} pole figure has two dots and the $\{10\bar{1}0\}$ has six. The number of markers is a result of crystal symmetry. As previously noted, the members of {1001} are (0001) and $(000\bar{1})$. The symmetrically equivalent members of $\{10\bar{1}0\}$ are $(10\bar{1}0)$, $(01\bar{1}0)$, $(0\bar{1}10)$, $(1\bar{1}00)$ and $(\bar{1}100)$.

A single pole figure shows the direction a specific plane-normal makes with respect to the sample normal, but it provides no information on the rotation about the plane-normal within the sample plane. However, using two pole figures the full 3D orientation can be derived as shown in the schematic in Fig. 2 for a single crystal. For a polycrystal, it is not so simple to interpret. Figure 3 shows a set of three pole figures for a rolled copper sheet sample with 2,600 grain orientations. While general trends in orientation can be observed in the pole figures, it is not possible to isolate a single grain and derive its orientation from such plots.

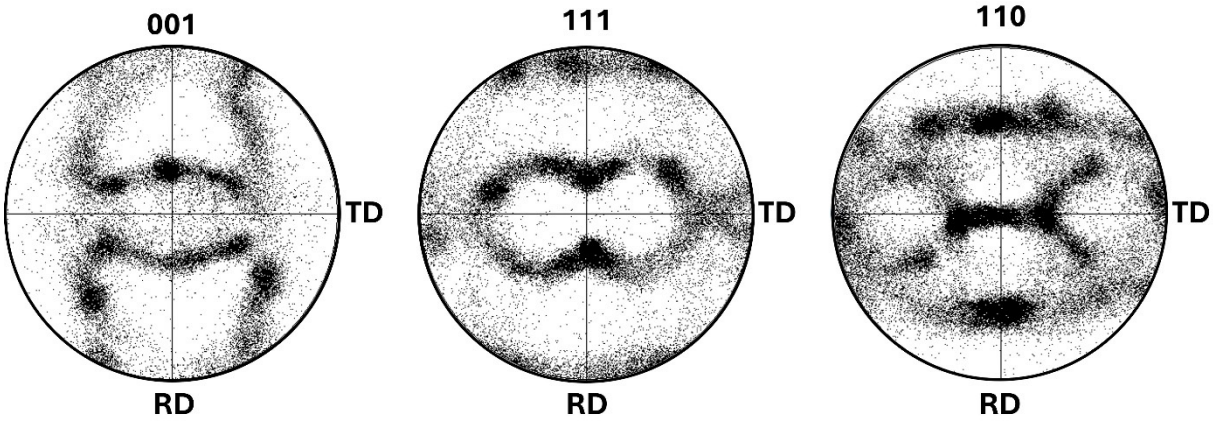

Figure 3. Pole figures for a set of EBSD measurements on rolled copper sheet. RD signifies the rolling direction and TD signifies transverse direction and the centre of the pole figure is the sheet normal or ND.

2.2. Inverse pole figures

Another tool complementary to the pole figure for describing the orientation of a crystal plane with respect to the sampling plane is the inverse pole figure. The inverse pole figure describes the plane-normal aligned with a specific sample direction (most commonly the sample normal direction or ND). Figure 4 shows a cubic crystal within a sample with a (111) crystal plane nearly parallel to the sample surface. The corresponding ND inverse pole figure is also shown.

Once again, the multiple dots are due to crystal symmetry. To simplify interpretation of the inverse pole figure, only an asymmetric region of the inverse pole figure is usually displayed. This is often termed the unit triangle (however, for other crystal symmetries the shape is often not triangular).

As with the pole figure, a single inverse pole figure provides information on the crystal plane-normal aligned with the inverse pole figure direction but provides no information on the rotation about the plane normal within the sample surface plane. Like pole figures, two inverse pole figures for orthogonal sample directions will give a full description of the orientation for a

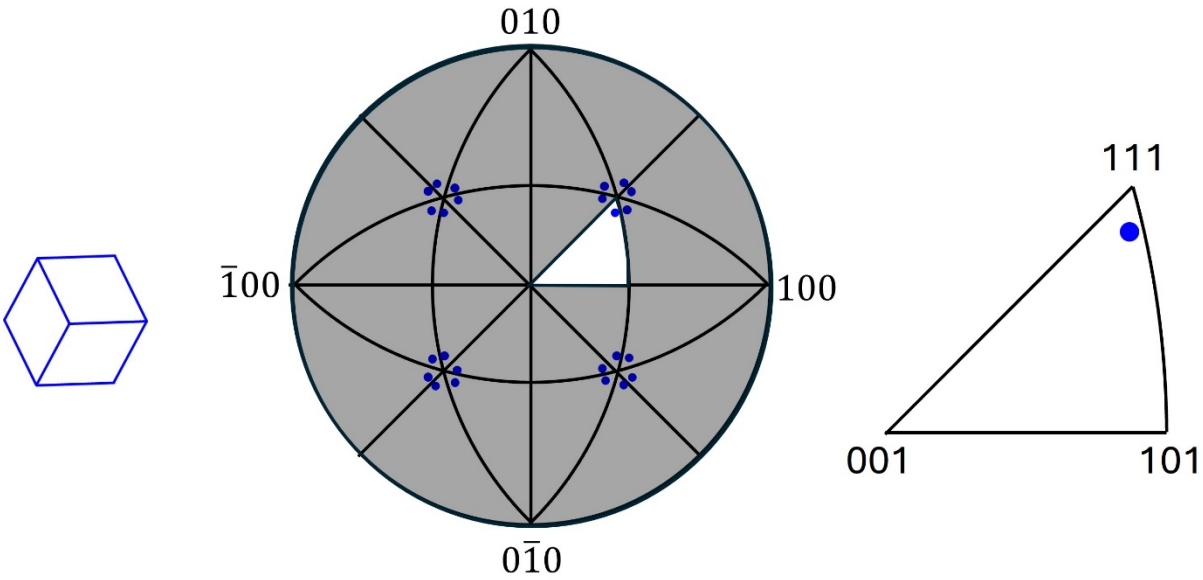

Figure 4. Normal direction (ND) inverse pole figure for a cubic crystal with the {111} crystal plane nearly parallel to the sample surface.

single crystal. However, the full orientation description of each individual crystal in a set of EBSD orientations in a polycrystal cannot be clearly differentiated from a set of inverse pole figures (see Fig. 5).

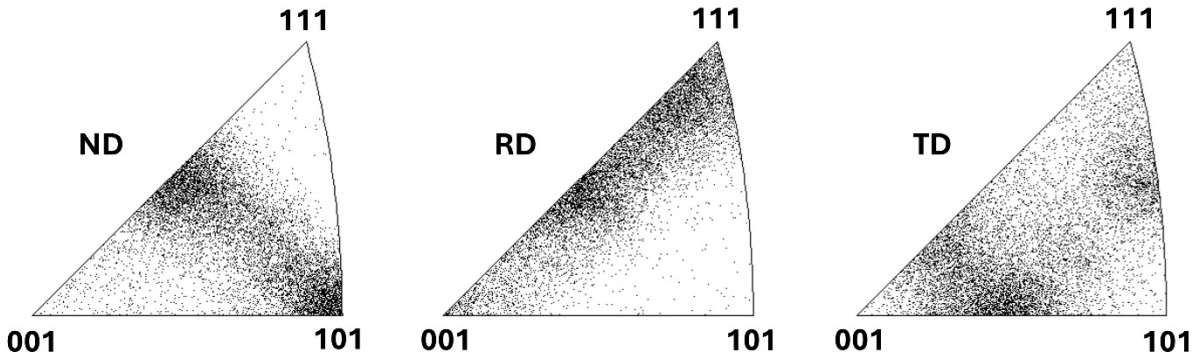

Figure 5. Inverse pole figures for a set of EBSD measurements in rolled copper sheet. ND signifies the sheet normal, RD the rolling direction and TD the transverse direction in the sheet.

2.3. Orientation colour mapping

The idea of colouring grains according to crystallographic orientation precedes EBSD [1, 2] but has really blossomed since the automation of EBSD. If we assign colours to the corners of the unit triangle [3] (e.g., red to (001), green to (110) and blue to (111)) and then construct smooth

gradients in colour between each corner then it is possible to map a colour to a point in a scan based on the (*hkl*) parallel to the sample surface at that point. Applying this colour scheme to each orientation measurement in an EBSD scan will then create a colour image (or map) as shown in Fig. 6. Other colour schemes can be employed. This technique is often referred to as orientation mapping or orientation imaging microscopy [4].

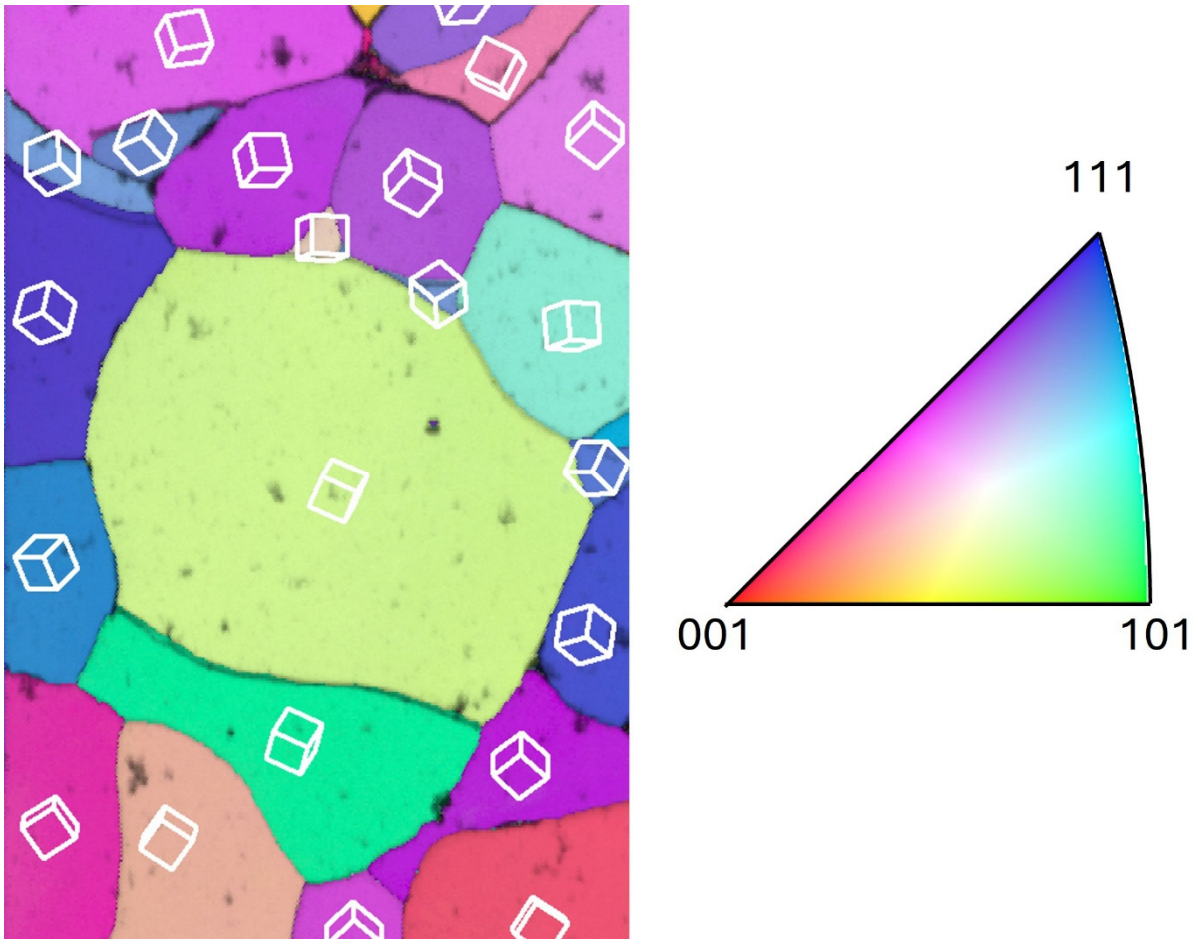

Figure 6. Orientation map showing alignment of crystal planes with respect to the sample surface.

2.4. Metallurgical notation {hkl}⟨uvw⟩

Often, just knowing the orientation of a specific crystallographic plane is not enough information. As previously noted, slip tends to happen on a limited set of lattice planes. However, not only does slip happen on particular planes but the direction of slip is also limited to specific crystallographic directions. For example, face-centred cubic materials tend to slip on {111} planes in $\langle 1\bar{1}0 \rangle$ directions. The slip system terminology points towards the need for a description of orientation sometimes referred to as metallurgical notation: {*hkl*}⟨*uvw*⟩. This notation describes the plane {*hkl*} parallel to the sample surface (the "3" direction in Fig. 7) and the crystal direction aligned with the "1" direction in the sample (E_1 in Figure 7). Note that the sample surface normal E_3 and the sample direction E_1 must be normal to each other.

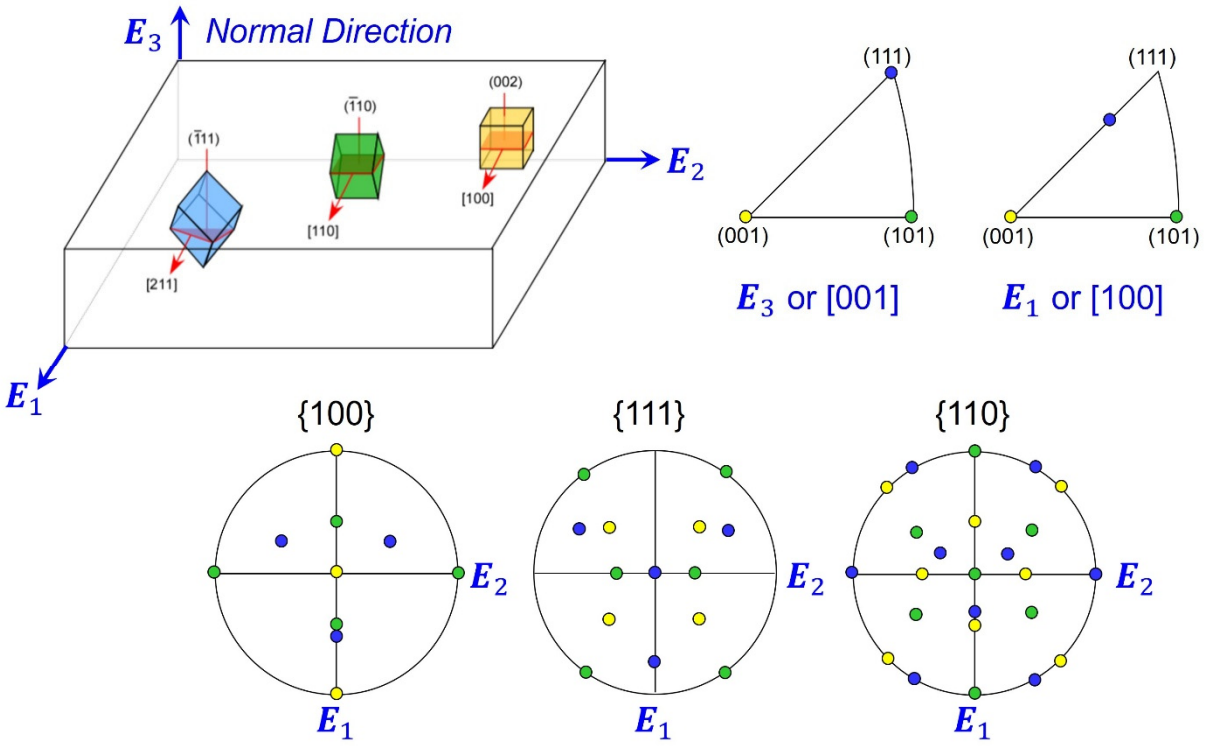

Figure 7. $(\bar{1}11)[211]$(-111), $(\bar{1}10)[110]$ (-110) and $(002)[100]$ oriented crystals shown in inverse pole figures and pole figures.

While metallurgical notation is helpful it is not a continuous description of orientation and only helpful for some specific well-understood orientations. For a full quantitative description of the three-dimensional crystallographic orientation needed for statistical treatment of orientation data, other orientation descriptions are needed. However, before proceeding both the sample and crystal reference frames must be clearly defined.

3. SAMPLE REFERENCE FRAME

The crystallographic orientation is, at its core, the set of rotations that bring the principal axes of the crystal into alignment with a specified reference frame [5]. Thus, a critical aspect of the orientation is the reference frame. The reference frame may be a combination of the sample, scanning electron microscope (SEM), and EBSD geometry – an example is shown in Fig. 8.

It is important to note that the sample reference frame will be affected in how the prepared specimen is obtained from the original sample. An easy example would be a coupon prepared from rolled sheet. One straightforward approach would be to prepare the sample such that the sheet normal is aligned with E_3 as shown in Fig. 2 and the rolling direction aligned with $E_1$and the transverse direction with E_2. However, if the sample was prepared by cross-sectioning

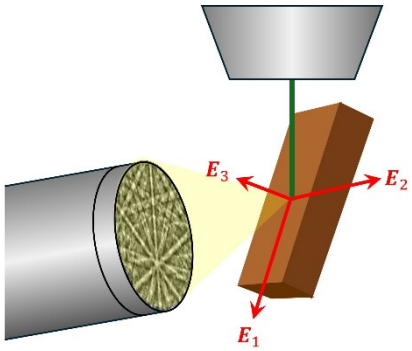

Figure 8. Sample EBSD reference frame.

normal to the rolling direction, then the rolling direction would be aligned with E_3, and the sheet normal generally aligned with E_1 or E_2. It is important to keep track of how the sample was prepared and mounted in the SEM sample holder relative to the EBSD detector.

Another important aspect of the sample reference frame is the direction of scanning in the microscope, i.e., is the horizontal direction of the scanning parallel to E_2 and/or the vertical direction of scanning aligned with positive E_1or negative E_1. Several possible geometries are shown in Fig. 9. This can be checked using a known sample such as a coin. This is often not critical for absolute measurements of crystallographic orientation but is critical for the correlation of crystallographic orientation with the orientation of boundary planes (i.e., boundary traces on a 2D section plane) or other microstructural features or when performing 3D measurements.

4. CRYSTAL REFERENCE FRAME

Just as the sample reference frame needs to be well defined, so does the crystal reference frame. For a crystal with cubic symmetry this is straight-forward. If we assume a right-handed reference frame given by the directions e_1, e_2 and e_3, then the for a cubic crystal the reference system is generally given as [001] (i.e., c) parallel to e_3, [100] (i.e., a) parallel to e_1 and [010] (i.e., b) parallel to e_2. This can also be described in shorthand as [001] || e_3, [100] || e_1 (the third axis must necessarily be [010] || e_2 and is excluded for brevity). However, for a cubic crystal, [001], [100] and [010] are all symmetrically equivalent. For tetragonal and orthorhombic crystals, the reference frame can still be given as [001] || e_3, [100] || e_1. But it is important to note that [001] || e_3, [100] || e_1 and [001] || e_3, [010] || e_1 would be two different reference frames as [001] and [010] are not symmetrically equivalent in crystals with orthorhombic point group symmetry.

For hexagonal symmetries, [0001] || e_3 is typical. However, two alternative settings for the hexagonal crystal reference frame are commonly used: [0001] || e_3, $[2\bar{1}\bar{1}0]$ || e_1 and [0001] || e_3, $[0\bar{1}10]$ || e_1 (see Fig. 10).

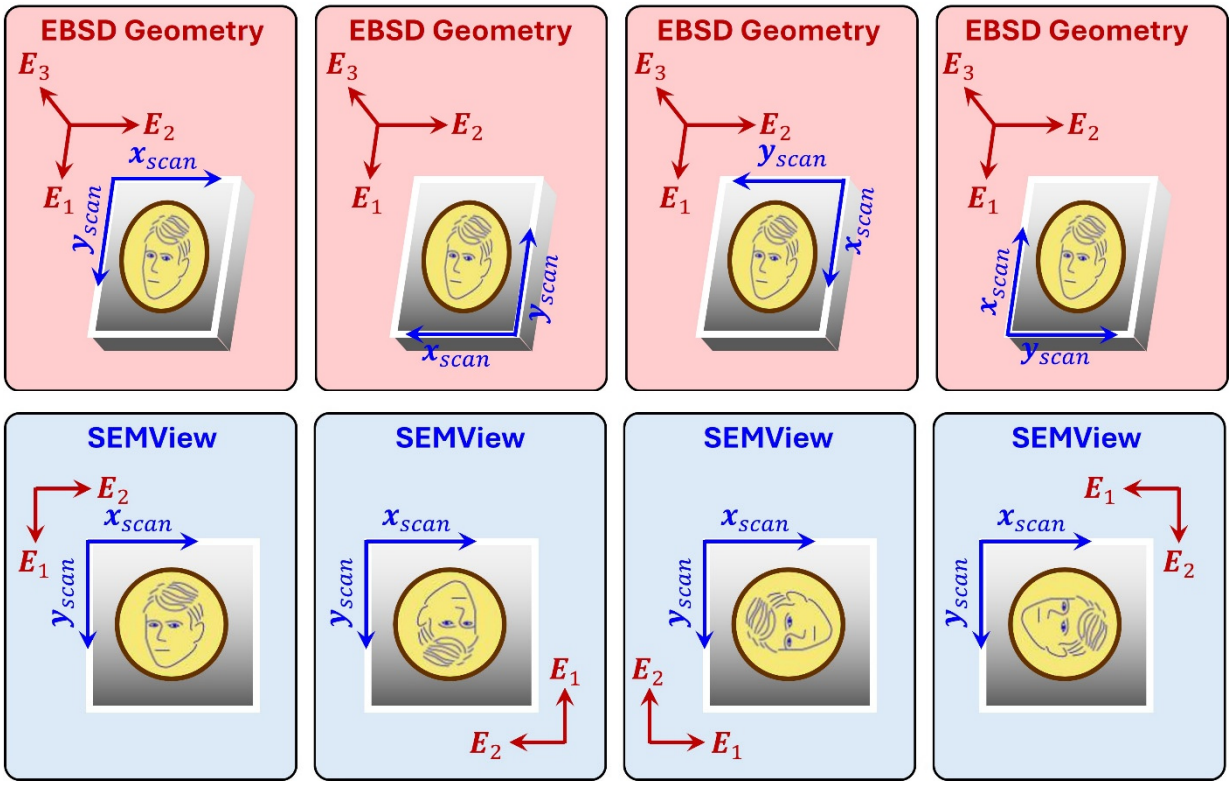

Figure 9. Scanning reference frame relative to the EBSD detector and as viewed on the SEM monitor.

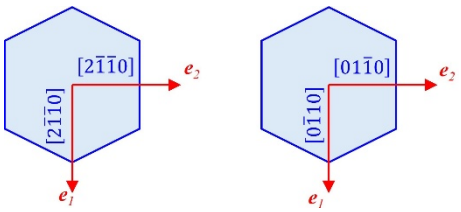

Figure 10. Two common settings for crystals with hexagonal symmetry.

For other crystal symmetries multiple settings may be used. We generally use $\vec{a} \parallel e_1$ and $\overrightarrow{c^*} \parallel e_3$ where c* is the c direction in reciprocal space. This can alternatively be written as $[100] \parallel e_1, (001) \parallel e_3$. However, $\vec{c} \parallel e_3, \overrightarrow{a^*} \parallel e_2$ and $\vec{c} \parallel e_3, \overrightarrow{b^*} \parallel e_2$ are also often used within the EBSD community. This definition should always be checked if absolute orientations are of interest. Especially, if comparing measurements on low symmetry materials where conventions often differ between metallurgists and geologists.

5. *OTHER ORIENTATION REPRESENTATIONS*

Before proceeding, we should note that there are two ways of considering orientations. (1) active – the rotation(s) needed to bring the crystal reference frame (e_1, e_2, e_3) into coincidence with the sample reference frame (E_1, E_2, E_3), and (2) passive – the rotation(s) to bring the sample reference frame into coincidence with the crystal reference frame. The passive approach is typically used in crystallographic texture analysis (i.e., the statistical analysis of crystallographic orientations).

5.1. Euler angles

Historically for the analysis of texture, Euler angles have been used to describe the three rotations to bring the sample reference frame into coincidence with the sample reference frame [6-8]. In Bunge notation, these three successive rotations are given as φ_1, Φ and φ_2. φ_1 is the rotation about the e_3 axis of the crystal, Φ is the rotation about the e_1 axis, and φ_2 is the rotation about the new e_3' axis. The ranges for these three rotations are $\varphi_1 \in [0, 2\pi], \Phi \in [0, \pi], \varphi_2 \in [0, 2\pi]$. Conventionally, orientations are plotted as sections through the space defined by the ranges of the three angles (or a sub-space depending on crystal symmetry) as shown in Fig. 11.

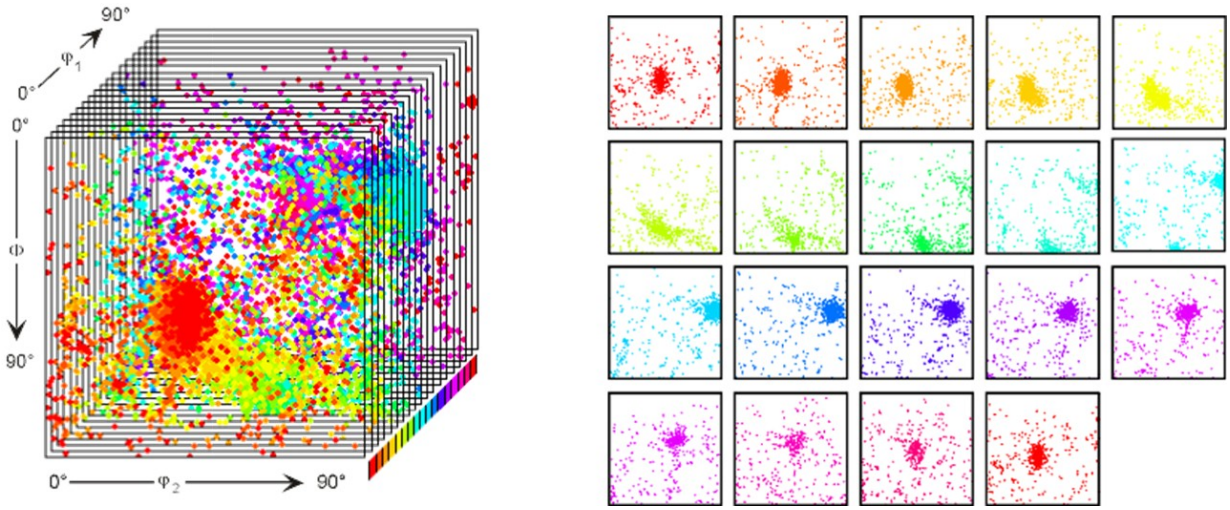

Figure 11. φ_1 sections through a discrete Euler space plot of a set of orientations.

One disadvantage of Euler angles is that they have a singularity as Φ approaches the range limits of 0 and π. At 0 and π, φ_1 and φ_2 are undefined. Another disadvantage is that Euler space is very much non-linear.

5.2. Rotation matrices

While rotation matrices do not lend themselves to graphical display, they can be useful in converting between different orientation representations [9] and for numerical analysis. The three successive rotations described by the Euler angle triplet φ_1, Φ and φ_2 can be given as a rotation matrix as follows:

$$g_{\varphi_1} = \begin{bmatrix} cos\varphi_1 & sin\varphi_1 & 0 \\ -sin\varphi_1 & cos\varphi_1 & 0 \\ 0 & 0 & 1 \end{bmatrix}, g_{\Phi} = \begin{bmatrix} 1 & 0 & 0 \\ 0 & cos\Phi & sin\Phi \\ 0 & -sin\Phi & cos\Phi \end{bmatrix}, g_{\varphi_2} = \begin{bmatrix} cos\varphi_2 & sin\varphi_2 & 0 \\ -sin\varphi_2 & cos\varphi_2 & 0 \\ 0 & 0 & 1 \end{bmatrix}$$

When these three matrices are multiplied the following product matrix is obtained.

$$g = \begin{bmatrix} cos\varphi_1 cos\varphi_2 - sin\varphi_1 sin\varphi_2 cos\Phi & sin\varphi_1 cos\varphi_2 + cos\varphi_1 sin\varphi_2 cos\Phi & sin\varphi_2 sin\Phi \\ -cos\varphi_1 sin\varphi_2 - sin\varphi_1 cos\varphi_2 cos\Phi & -sin\varphi_1 sin\varphi_2 + cos\varphi_1 cos\varphi_2 cos\Phi & cos\varphi_2 sin\Phi \\ sin\varphi_1 sin\Phi & -cos\varphi_1 sin\Phi & cos\Phi \end{bmatrix}$$

The same matrix can be constructed using the metallurgical notation $\{hkl\}\langle uvw\rangle$:

$$g = \begin{bmatrix} u & r & h \\ v & s & k \\ w & t & l \end{bmatrix}$$

Or as an axis of rotation $\boldsymbol{d} = (d_1, d_2, d_3)$ and angle of rotation ω:

$$g = \begin{bmatrix} (1 - {d_1}^2)cos\omega + {d_1}^2 & d_1 d_2(1 - cos\omega) + d_3 sin\omega & d_1 d_3(1 - cos\omega) - d_2 sin\omega \\ d_1 d_2(1 - cos\omega) - d_3 sin\omega & (1 - {d_2}^2)cos\omega + {d_2}^2 & d_2 d_3(1 - cos\omega) + d_1 sin\omega \\ d_1 d_3(1 - cos\omega) + d_2 sin\omega & d_2 d_3(1 - cos\omega) - d_1 sin\omega & (1 - {d_3}^2)cos\omega + {d_3}^2 \end{bmatrix}$$

This will become of more interest in the discussion on misorientation.

5.3. Quaternions

Quaternions [10] have the same advantages of rotation matrices for numerical manipulations but are less memory intensive as they have only four components as compared to nine for matrices and computationally more efficient in calculating quaternion products as compared to matrix products. Modern computer codes for analysing orientation tend to use quaternions as opposed to orientation matrices.

5.4. Rodrigues-Frank vectors

Another representation of interest is the Rodrigues-Frank vector [11]. The Rodrigues-Frank vector combines the axis-angle ($\boldsymbol{d}$, ω) representation introduced in the orientation matrices section into a single vector. The rotation axis is converted to a unit vector n^ and the Rodrigues-Frank vector is then given by:

$$\rho = \hat{\boldsymbol{n}} \tan\frac{\omega}{2}$$

These vectors lack the singularity of Euler angles. However, for lower crystal symmetries care must be taken when $\omega \geq \pi$.

As the space of 3D rotations (SO3) is inherently non-linear, Rodrigues-Frank space is also non-linear. However, one advantage of Rodrigues-Frank space is that locally, it behaves linearly.

For optimal sampling of orientation space, it is helpful to have a parameterisation that is as close to linear as possible. The cubochoric approach which is related to the Rodrigues-Frank vector has been found to be helpful for uniformly sampling orientation space [12] and can also be used for visualizing orientations [13] although such visualisations are still relatively uncommon in the EBSD community.

6. MISORIENTATION

Misorientations are similar to orientations, but instead of bringing the crystal lattice into coincidence with the sample reference frame, a misorientation refers, instead, to bringing the crystal lattice of one grain into coincidence with the crystal lattice of another grain.

6.1. Axis/angle

For any two crystal lattices of different orientation, there exists an axis common to both lattices. Two parameters are needed to describe the orientation of the common axis with respect to the crystal reference frame. However, three parameters are generally used, i.e., [*uvw*] but two angles could be used instead. A third parameter is needed to describe the rotation about this common axis to bring the two crystal lattices into coincidence. Misorientations are most commonly described using axis/angle pairs, but misorientation can be represented as Euler angles or Rodrigues-Frank vectors as well. The example in Fig. 12 shows the misorientation as an axis/angle pair - a 45° rotation about the [100] crystal axis will bring the two cubes into coincidence.

As with the crystal planes and directions, the point group symmetry of the crystal will have an impact on the misorientation. For example, Table 1 shows the symmetric equivalents for the 45° rotation about [100] shown in Fig. 12.

The terms "misorientation" and "disorientation" are sometimes used interchangeably. However, the term "disorientation" is the misorientation with the minimum rotation angle out of all the symmetrically equivalent misorientations. For the example in Table 1, this would be the 45° rotation about the <001> axis. The term "disorientation" as used in the literature may also simply refer to the minimum angle.

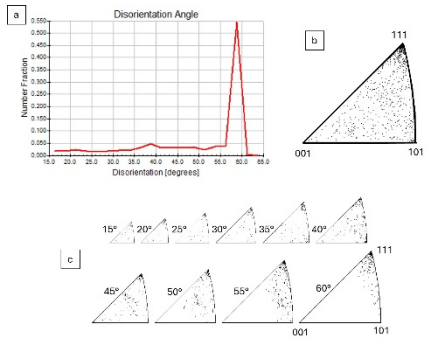

Figure 12. Schematic of the misorientation at a grain boundary for a cubic crystal.

Table 1. List of symmetrically equivalent axis/angle pairs for a 45° rotation about [100].

Angle	Axis
45.0°	⟨001⟩
98.4°	⟨225⟩
135.00°	⟨001⟩
148.6°	⟨525⟩
180.0°	⟨205⟩
211.4°	⟨525⟩
225.0°	⟨001⟩
261.6°	⟨225⟩
315.0°	⟨001⟩

It should be noted that the axis/angle pair is simply a mathematical description. It does not necessarily mean that two neighbouring orientations in an EBSD scan physically rotated with respect to one another as described by the axis/angle pair during the forming process.

Axis/angle pairs can be examined independently or together as illustrated in Fig. 13 for EBSD data obtained from a heavily twinned copper sample. The twin relationship formed during recrystallisation of copper is a 60° rotation about <111>. A cluster of points can be observed at 60° in the disorientation angle distribution shown in Fig. 13a and at <111> position in the disorientation axis plot in Fig. 13b and at the 60° @ <111> location in the axis/angle distribution in Fig. 13c.

As with other parameterisations of 3D rotations, axis/angle space is also non-linear. The sections through axis/angle space shown in Fig. 14c give an approximation of this non-linearity.

Note that for misorientations, the sample reference frame is no longer relevant. However, if the orientation of the boundary plane (or trace of the boundary plane in a 2d planar section) is to be coupled with misorientation at the boundary then knowledge of the sample reference frame is necessary.

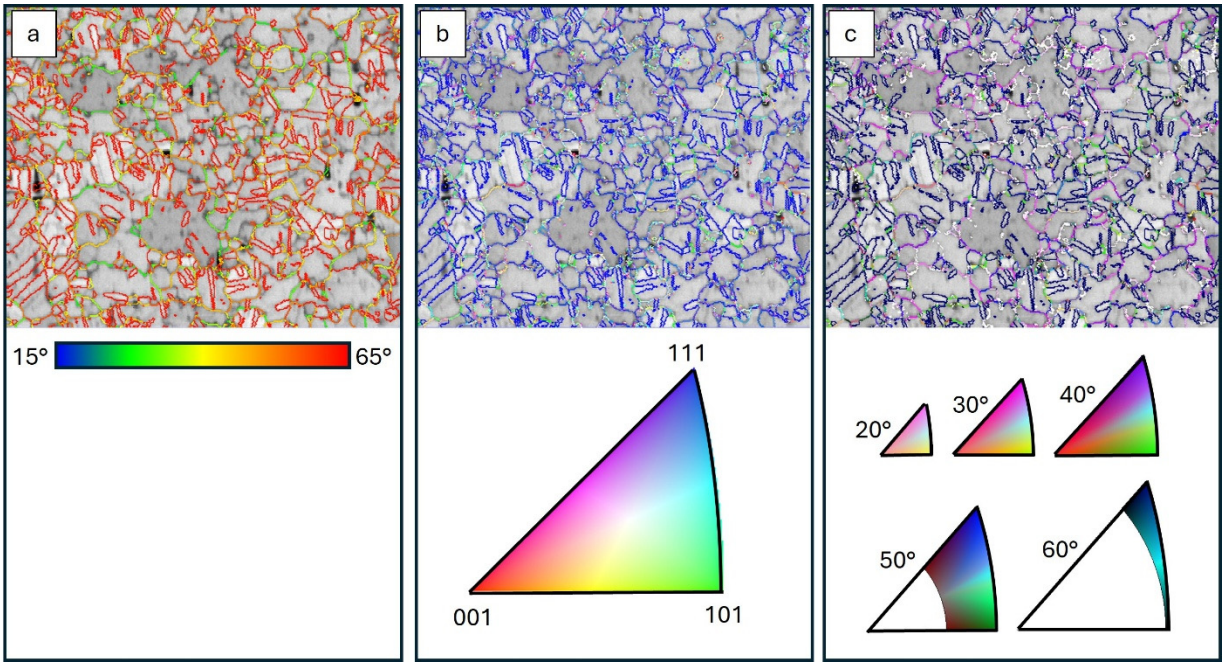

Figure 13. Disorientations in a heavily twinned copper sample. a) Distribution of disorientation angles; b) Distribution of disorientation axes in an inverse pole figure; and c) sections through axis/angle space.

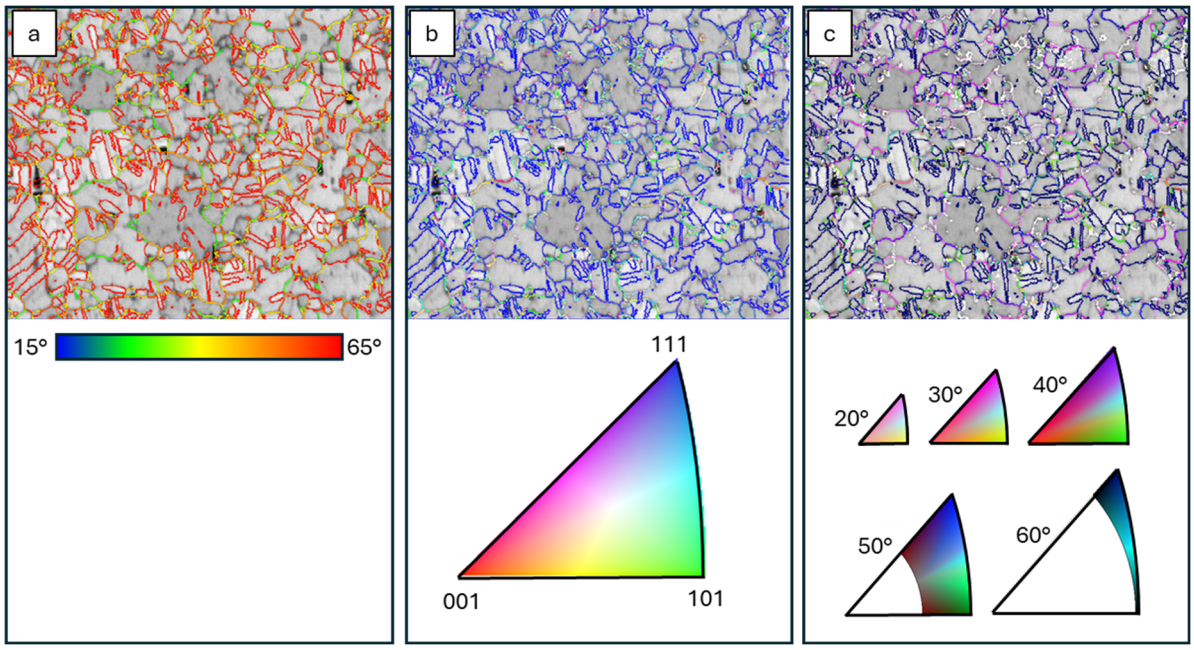

Figure 14 Boundaries coloured according to disorientation in a heavily twinned copper sample. a) Disorientation angle boundaries, b) disorientation axis boundaries, and c) combined disorientation axis/angle boundaries [15].

6.2. Rodrigues-Frank vector

Misorientations can also be plotted in Rodrigues-Frank space as shown in Figure 15. Notice the large cluster at the edge of the domain along the [111] direction. This is due to the rotation of 60° about <111> for the recrystallisation twins (the maximum disorientation in a cubic crystal is 62.8°, 60° when the disorientation axis is <111>). The domain for orientations for cubic crystals is a truncated cube and the domain for misorientations is a truncated prism (Heinz and Neumann, 1991).

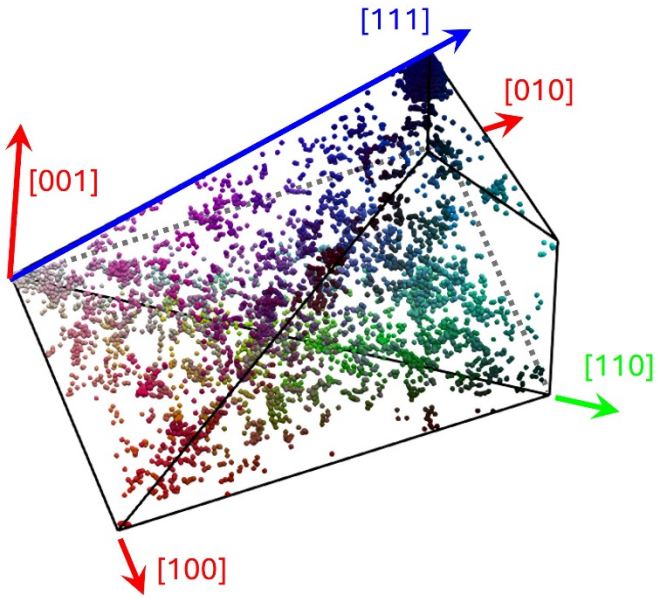

Figure 15. Disorientations for a heavily twinned nickel sample plotted in Rodrigues space. Colours follow those in [15].

7. REFERENCES

[1] Sander B 1950 *Einführung in die Gefügekunde der geologischen Körper*. [Vienna, Austria: Springer Verlag]

[2] Wenk H-R 1965 *Mineralogische u. Petrographische Mitteilungen* **45** 467-515

[3] Inokuti Y, Maeda C and Ito Y 1986 *J. Japan. Inst. Metals* **50** 874-878

[4] Adams B L, Wright S I and Kunze K 1993 *Metallurg. Trans. A* **24** 819-831

[5] Britton T, Jiang J, Guo Y, Vilalta-Clemente A, Wallis D, Hansen L N, Winkelmann A and Wilkinson A 2016 *Mater. Characterization* **117** 113-126

[6] Roe R-J 1966 *J. Appl. Phys.* **37** 2069-2072

[7] Bunge H-J 1982 *Texture analysis in materials science. Mathematical methods*. [London, U.K.: Butterworths]

[8] Kocks U F, Tome C N and Wenk H-R (Eds.) 1998. *Texture and anisotropy*. [Cambridge, U.K.: Cambridge University Press]

[9] Rowenhorst D, Rollett A D, Rohrer G S, Groeber M, Jackson M, Konijnenberg P J and De Graef M 2015 *Modell. Simul. Mater. Sci. Eng.* **23** 083501
[10] Hamilton W R 1844 *On Quaternions; or on a new system of imaginaries in Algebra*. [London, Edinburgh and Dublin: Philosophical Magazine and Journal of Science]
[11] Frank F C 1988 *Metallurg. Trans. A* **19** 403-408
[12] Singh S and De Graef M 2016 *Modell. Simul. Mater. Sci. Eng.* **24** 085013
[13] Callahan P G, Echlin M, Pollock T M, Singh S and De Graef M 2017 *J. Appl. Crystall.* **50** 430-440
[14] Heinz A and Neumann P 1991 *Acta Crystallogaphica A* **47** 780-789
[15] PAatala S and Schuj C A 2011 *Acta Materialia* **59** 554-562